Second International Congress on Technology, Communication and Knowledge (ICTCK 2015) November, 11-12, 2015 - Mashhad Branch, Islamic Azad University, Mashhad, Iran

LMI-based Robust Constrained Model Predictive control of Two-Wheeled Inverted Pendulum

Niloufar Minouchehr
Department of Electrical Engineering
Ferdowsi University of Mashhad
Mashhad,Iran
niloofar_minoochehr@stu.um.ac.ir

Seyyed Kamal Hosseini-Sani
Department of Electrical Engineering
Ferdowsi University of Mashhad
Mashhad,Iran
k.hosseini@um.ac.ir

Nima Vaezi
Department of Electrical Engineering
Ferdowsi University of Mashhad
Mashhad,Iran
nimavaezi368@gmail.com

Parisa Tavakoli
Department of Electrical Engineering
Ferdowsi University of Mashhad
Mashhad,Iran
parisatavakoli@yahoo.co.uk

Abstract— **Two-Wheeled Inverted Pendulum (TWIP) robot is considered as an unstable and underactuated system affected by physical and environmental constrains. In addition, due to the model uncertainties, a robust control approach is needed to stabilize the posture of the TWIP. Robust Model Predictive Control (RMPC) based on linear matrix inequality (LMIs) is addressed to an optimization problem of the "worst-case" objective function over infinite moving horizon, subject to input and output constraints. In this paper, LMI-based RMPC is applied to a TWIP in spite of model uncertainty and motor torque constraint. A parametric poly-topic uncertainty model is used to describe the robot. Maximum torque produced by motors is defined as control input constraint. The efficiency of the RMPC is verified by comparing with nominal MPC.**

I. INTRODUCTION

Two-Wheeled Inverted Pendulum (TWIP) is addressed to a robot balanced on two wheels. The fundamental model of a TWIP has been utilized to stabilize the posture of various applications such as Segway HT, Segway RMP and automatic wheelchairs. The control objective is to make the tilt angle converge to zero to balance the system. Dynamic model of a TWIP is describe by two decouple subsystems that can be independently controlled [1, 2].

Control of a TWIP has been considered as such a challenging issue due to its inherently unstable dynamics. In addition, it is regarded as an underactuated system which the number of control inputs is less that its degrees of freedom to be stabilized. Moreover, it is exposed to input constrains, that is, maximum torque produced by motors. Therefore, it is necessary to use a robust controller to achieve the control objectives[1, 3, 4].

Many control techniques have been studied in the past decade for the control of TWIP robot. In [5, 6] adaptive pole placement is utilized to get an appropriate performance of TWIP. Linear Quadratic Regulator (LQR) is another controller applied on TWIP as presented in [7]. Both of latter methods perform weakly in the presence of uncertainties. Sliding mode controllers used in [3, 4, 8] show robust performance against parameter variations and uncertain disturbances. Intelligent techniques have been used to improve the performance of the system, as in [9-11].

Model Predictive Control is a control strategy that uses an explicit model of the processes to optimize the performance of the system. In [12], a Deterministic Autoregressive Moving Average (DARMA) model of TWIP is used. In [13] , by the use of a linear state space of TWIP, two MPC controllers are designed. The purpose of this paper is to show that the robust MPC can be successfully applied to balance a TWIP. The advantages of the RMPC stems from the possibilities to consider input and output constrains in addition to model uncertainties [14]. In a TWIP, model uncertainties can be arisen due to the different mass and height of the pendulum that can cause uncertainties in

The paper is organized as follows. Section II presents a dynamic model of a TWIP Newton–Euler approach. Section III is devoted to describe LMI-based RMPC algorithm. The simulation results of the RMPC applied on a TWIP are presented in Section V. Furthermore, comparison of the

978-1-4673-9762-9/15/$31.00 ©2015 IEEE

RMPC with a LQR is brought in this part to show the validity of the proposed approach. Section V presents the conclusions from the study.

II. DYNAMIC MODEL

In this section, mathematical model of a TWIP using Newton–Euler approach is presented. As depicted in Fig.1, the TWIP consists of two independent actuators (brushless motors) which provide the torques to the wheels to stabilize the robot as well as rotate around the *z*-axis. The table of forces and moments affecting the vehicle is shown in in Table I.

The control objective is to make the heading angle θ, and the tilt angle converge to desired values, θ_d and zero, respectively [2]. The essential idea is to use the pitch angle α as a "gas pedal" for the vehicle and use it to accelerate and decelerate until the specified speed is attained [15].

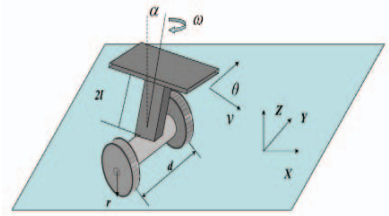

Figure 1. Model of Two-Wheeled Inverted Pendulum [1]

TABLE I. PARAMETERS OF TWIP ROBOT

F_l, F_r	Interacting forces between the left and right wheels and the platform
H_l, H_r	Friction forces acting on the left and right wheels
τ_l, τ_r	Torques provided by wheel actuators acting on the left and right wheels
d_l, d_r	External forces acting on the left and right wheels
θ_l, θ_r	Rotational angles of the left and right wheels
x_l, x_r	Displacements of the left and right wheels along the *x*-axis
α	Tilt angle of the pendulum
θ	Heading angle of the vehicle
M_w	Mass of the wheel
I_w	Moment of inertia of the wheel with respect to the *y*-axis
r	Radius of the wheel
m	Mass of the pendulum
g	Gravity acceleration
l	Distance from the point O to the center of gravity, CG, of the pendulum
d	Distance between the left and right wheels along the *y*-axis
M	Mass of the platform
I_M	Moment of inertia of the platform about the *y*-axis
I_P	Moment of inertia of the platform and pendulum about the *z*-axis
F_p	Interacting force between the pendulum and the platform on the *x*-axis
M_p	Interacting moment between the pendulum and the platform about the *y*-axis
v	the forward velocity of the mobile platform

With an assumption that there is no slip between the wheels and the ground, balancing forces and moments acting on the left wheel results in the following equations of motion of the left wheel, as in

$$I_w\ddot{\theta}_l = F_l - H_l r \tag{1}$$

$$M_w\ddot{x}_l = d_l - F_l + H_l \tag{2}$$

Similarly, for the right wheel we have

$$I_w\ddot{\theta}_r = F_r - H_r r \tag{3}$$

$$M_w\ddot{x}_r = d_r - F_r + H_r \tag{4}$$

Balancing forces acting on the pendulum on the *x*-axis direction and moments about the center point of gravity O results in (5, 6).

$$-ml\cos(\alpha)\ddot{\alpha} + ml\dot{\alpha}^2\sin(\alpha) - m\ddot{x} = F_p \tag{5}$$

$$ml^2\ddot{\alpha} + ml\cos(\alpha)\ddot{x} - mgl\sin(\alpha) = M_p \tag{6}$$

where ml^2 is the moment of inertia of the pendulum with respect to the *y*-axis.

Balancing forces acting on the platform along the x-axis direction, and moments about the z-axis results in

$$M\ddot{x} = F_l + F_r + F_p \tag{7}$$

$$I_M\ddot{\alpha} = -M_p \tag{8}$$

Balancing the moments acting on the platform and pendulum about the *z*-axis gives

$$I_P\ddot{\theta} = d(F_l - F_r) \tag{9}$$

A calculation, from (1) to (9) gives the following set of equations of motion of the two wheeled mobile vehicle with an inverted pendulum, as in

$$\ddot{\theta} = \frac{d}{2rI_\theta}(\tau_l - \tau_r) + \frac{d}{2I_\theta}(d_l - d_r) \tag{10}$$

$$\ddot{x} = \frac{1}{\Omega_0}\left[I_\alpha ml\sin(\alpha)\dot{\alpha}^2 - m^2l^2g\sin(\alpha)\cos(\alpha)\right] + \frac{I_\alpha(\tau_l + \tau_r)}{\Omega_0 r} + \frac{I_\alpha(d_l + d_r)}{\Omega_0} \tag{11}$$

$$\ddot{\alpha} = \frac{1}{\Omega_0}\left[M_x mgl\sin(\alpha) - m^2l^2\cos(\alpha)\sin(\alpha)\dot{\alpha}^2\right] - \frac{ml\cos(\alpha)(\tau_l + \tau_r)}{\Omega_0 r} - \frac{ml\cos(\alpha)(d_l + d_r)}{\Omega_0} \tag{12}$$

where

$$
\begin{aligned}
I_\theta &= I_p + \frac{d^2}{2}\left(\frac{I_w}{r^2} + M_w\right) \\
I_\alpha &= mL^2 + I_M \\
M_x &= M + m + 2\left(\frac{I_w}{r^2} + M_w\right) \\
\Omega_0 &= M_x I_\alpha - m^2 l^2 \cos(\alpha)^2
\end{aligned} \tag{13}
$$

Now, it is needed to linearize the result around the operating point, $\alpha = \dot{\alpha} = 0$ and $\theta = \dot{\theta} = 0$. We define 5-dimensional vector of state variables as $\begin{bmatrix} \alpha & \dot{\alpha} & v & \theta & \dot{\theta} \end{bmatrix}^T$. The system's state space equations can be written in matrix form as in (14).

$$
\begin{bmatrix} \dot{x}_1 \\ \dot{x}_2 \\ \dot{x}_3 \\ \dot{x}_4 \\ \dot{x}_5 \end{bmatrix} = \begin{bmatrix} 0 & 1 & 0 & 0 & 0 \\ t_1 & 0 & 0 & 0 & 0 \\ t_2 & 0 & 0 & 0 & 0 \\ 0 & 0 & 0 & 0 & 1 \\ 0 & 0 & 0 & 0 & 0 \end{bmatrix} \begin{bmatrix} x_1 \\ x_2 \\ x_3 \\ x_4 \\ x_5 \end{bmatrix} + \begin{bmatrix} 0 & 0 \\ t_3 & 0 \\ t_4 & 0 \\ 0 & 0 \\ 0 & t_5 \end{bmatrix} \begin{bmatrix} u_1 \\ u_2 \end{bmatrix} \tag{14}
$$

where

$$
t_1 = \frac{M_x mgl}{\Omega_0}, t_2 = \frac{-m^2 l^2 g}{\Omega_0}, t_3 = -\frac{ml}{\Omega_0 r}, t_4 = \frac{I_\alpha}{\Omega_0 r}, t_5 = \frac{d}{2rI_\theta} \tag{15}
$$

and

$$
\begin{aligned}
u_1 &= (\tau_l + \tau_r) \\
u_2 &= (\tau_l - \tau_r)
\end{aligned} \tag{16}
$$

The coefficients in the matrices in (14) are constant but known [1].

By the use of a decoupling unit transforming τ_α and τ_θ into the wheel torques τ_r and τ_l, we can control the rotation around the *z*-axis independently of the rotation around the *y*-axis [5]. Such a decoupling unit can be considered as

$$
\begin{aligned}
\tau_\alpha &= \tau_l + \tau_r \\
\tau_\theta &= \tau_l - \tau_r
\end{aligned} \tag{17}
$$

Therefore, the state space model (14) of the vehicle consists of two decoupled subsystems. The first is a ''pendulum'' system shown in (18), with $\begin{bmatrix} \alpha & \dot{\alpha} & v \end{bmatrix}^T$ as state parameters and $\tau_\alpha = \tau_l + \tau_r$ as input control.

$$
\begin{bmatrix} \dot{\alpha} \\ \ddot{\alpha} \\ \dot{v} \end{bmatrix} = \begin{bmatrix} 0 & 1 & 0 \\ t_1 & 0 & 0 \\ t_2 & 0 & 0 \end{bmatrix} \begin{bmatrix} \alpha \\ \dot{\alpha} \\ v \end{bmatrix} + \begin{bmatrix} 0 \\ t_3 \\ t_4 \end{bmatrix} \tau_\alpha \tag{18}
$$

and the second subsystem is ''rotation'' system with $\begin{bmatrix} \theta & \dot{\theta} \end{bmatrix}^T$ as state parameters and $\tau_\theta = \tau_l - \tau_r$ as input control, as in (19).

$$
\begin{bmatrix} \dot{\theta} \\ \ddot{\theta} \end{bmatrix} = \begin{bmatrix} 0 & 1 \\ 0 & 0 \end{bmatrix} \begin{bmatrix} \theta \\ \dot{\theta} \end{bmatrix} + \begin{bmatrix} 0 \\ t_5 \end{bmatrix} \tau_\theta \tag{19}
$$

We assume that the state variables are measured and available [1].

Now, we intend to design two independent controllers using RMPC strategy.

III. LMI-BASED MODEL PREDECTIVE CONTROL

Before The LMI-based RMPC utilized in this paper is based on that created in [14]. The type of model considered in this paper is discrete and linear time-invariant with the form of state space as (20).

$$
\begin{aligned}
&x(k+1) = A(k)x(k) + B(k)u(k) \\
&y(k) = Cx(k) + Du(k) \\
&\begin{bmatrix} A(k) & B(k) \end{bmatrix} \in \Omega
\end{aligned} \tag{20}
$$

where $u(k) \in \mathbb{R}^{n_u}$ is the control input, $x(k) \in \mathbb{R}^{n_x}$ is the state of the plant , $y(k) \in \mathbb{R}^{n_y}$ is the plant output and Ω is some prespecified set. For poly-topic systems, the set Ω is the poly-tope:

$$
\Omega = Co\left\{\begin{bmatrix} A_1 & B_1 \end{bmatrix}, \begin{bmatrix} A_2 & B_2 \end{bmatrix}, \cdots, \begin{bmatrix} A_L & B_L \end{bmatrix}\right\}, \tag{21}
$$

where Co denotes the convex hull. In other words, if $\begin{bmatrix} A & B \end{bmatrix} \in \Omega$, then for some nonnegative $\lambda_1, \lambda_2, ..., \lambda_L$ summing to one, we have:

$$
\begin{bmatrix} A & B \end{bmatrix} = \sum_{i=0}^{L} \lambda_i \begin{bmatrix} A_i & B_i \end{bmatrix} \tag{22}
$$

The system is described by (20) with the associated uncertainty set Ω. The purpose of RMPC is to find the control sequence $u(k+i \mid k), i = 0, 1, ..., m$ minimizing the robust performance objective as (22), at each sampling time *k*,

$$
\min_{u(\mathrm{k+i|k}),\mathrm{i}=0,1,\ldots,m} \max_{\begin{bmatrix} A(k+i) & B(k+i) \end{bmatrix} \in \Omega, i \geq 0} J_\infty(k) \tag{23}
$$

subject to

$$
\max_{i \geq 0} \left\| u_j(k+i \mid k) \right\| \leq u_{j,\max} \quad j = 1, 2, ..., n_u \tag{24}
$$

$$
\max_{\begin{bmatrix} A(k+j) & B(k+j) \end{bmatrix} \in \Omega, j \geq 0} \left\| y(k+i \mid k) \right\| \leq y_{\max} \quad i \geq 1 \tag{25}
$$

where

$$
J_\infty(k) = \sum_{i=0}^{\infty} \left(x(k+i \mid k)^T Q_1 x(k+i \mid k) + u(k+i \mid k)^T R u(k+i \mid k) \right) \tag{26}
$$

where Q_1 and R are symmetric positive definite weighting matrices.

An alternative technique to solve this "min-max" optimal problem is to define an upper bound (γ) on the worse-case objective function ($J_\infty(k)$). Assume that there are no constraints on the control input and plant output. Minimization of the upper bound with a constant state feedback control law $u(k+i\,|\,k) = Fx(k+i\,|\,k), i \geq 0$, at sampling time k, gives:

$$F = YQ^{-1} \tag{27}$$

where $Q > 0$ and Y are obtained from the solution (if it exists) of the following linear objective minimization problem:

$$\min_{\gamma,Q,Y} \gamma \tag{28}$$

subject to

$$\begin{bmatrix} 1 & x(k\,|\,k)^T \\ x(k\,|\,k) & Q \end{bmatrix} \geq 0 \tag{29}$$

and

$$\begin{bmatrix} Q & QA_j^T + Y^T B_j^T & QQ_1^{1/2} & Y^T R^{1/2} \\ A_j Q + B_j Y & Q & 0 & 0 \\ Q_1^{1/2} Q & 0 & \gamma I & 0 \\ R^{1/2} Y & 0 & 0 & \gamma I \end{bmatrix} \geq 0, \quad j = 1,2,...,L \tag{30}$$

The Euclidean norm constraints on control inputs and outputs described as (24) and (25) are guaranteed by LMIs in (31, 32).

$$\begin{bmatrix} {u_{\max}}^2 I & Y \\ Y^T & Q \end{bmatrix} \geq 0, \quad \text{with } {u_{\mathrm{j,max}}}^2 \geq X_{jj}, j = 1,2,...,n_u \tag{31}$$

$$\begin{bmatrix} Q & (A_j Q + B_j Y)^T C^T \\ C(A_j Q + B_j Y) & {y_{\max}}^2 I \end{bmatrix} \geq 0, j = 1,2,...,L \tag{32}$$

IV. Results And Analysis

The optimization problem is solved in the MATLAB programming environment using CVX toolbox [16]. The control objective is to make tilt angle α and rotation angle θ converge to zero and θ_d in order to stabilize the posture of the robot, in spite of model uncertainties and disturbances. The

According to (14) and (15), model of TWIP is dependent to variables that can cause model uncertainties. Some of these uncertainties are the mass and height of the person standing on the robot. In addition, the moments of inertia about axes cannot be precisely determined. Therefore, the model uncertainties are considered as following:

$$\begin{aligned} &40kg \leq m \leq 100kg, 0.7m \leq l \leq 1m \\ &\bar{I}_w = I_w \pm \%10 I_w, \\ &\bar{I}_M = I_M \pm \%10 I_M, \\ &\bar{I}_P = I_P \pm \%10 I_P \end{aligned} \tag{33}$$

where m is the mass of the pendulum and l is the distance from the center of gravity of the pendulum to the center of the chasis (considered as $\frac{1}{2}$ height of the the person standing on the robot). Other parameters of the model considered to be constant as Table II. By the combination of boundary values of uncertain parameters an uncertain system with parametric poly-topic uncertainty is given as in (21) with L=1,2,..,16. The nominal model is calculated for the mean values of the uncertain parameters.

Using decoupling unit, TWIP can be independently controlled by two RMPC. The controller must be robust enough to stabilize the posture of the TWIP, meanwhile rotate as desired, in spite of the model uncertainties, disturbances and constraints.

The objective function is defined as (26) and the weighting matrices for "pendulum" and "rotation" subsystems are chosen as following respectively

$$Q_{1\alpha} = \begin{bmatrix} 100 & 0 & 0 \\ 0 & 100 & 0 \\ 0 & 0 & 100 \end{bmatrix}, R_\alpha = 0.01 \tag{34}$$

$$Q_{1\theta} = \begin{bmatrix} 100 & 0 \\ 0 & 10 \end{bmatrix}, R_\theta = 0.01 \tag{35}$$

These weighting matrices have been selected so that the best performance in terms of setteling time and the minimization of the control input can be achieved. Fig.2 indicates the block diagram of the RMPC uses to stabilize the posture of the TWIP.

To show the robustness of RMPC against model uncertainties, its performance is compared with nominal MPC. The results of simulation of "pendulum" subsystem for $[\alpha \quad \dot{\alpha} \quad v \quad \theta \quad \dot{\theta}]$= [0.1750 0.0175 1 0 0] as initial condition for nominal system with no constraints are indicated in Figs 3 and 4. As shown in Fig.3 tilt angle and its rate converges to zero in less than 3 seconds with the use of both controllers. The maximum velocity needed for this activity is less than 3 m/s. The comparison of these controllers is shown in Tabale III for the nominal system and 8 vertexes of poly-topic model. As can be seen, the performance of both controllers is approximately the same for the nominal system, whilst RMPC stabilizes the TWIP with less MSE compared to MPC for the vertices of the model. In the other words, there are not much differences between nominal system and vertices of the poly-topic system of the RMPC performance. Nominal MPC has the best performance just for the case of nominal system that is designed for but the difference marginally increases when the system comes out the nominal point. Therefore, RMPC shows a robust performance against model uncertainties.

As mentioned before, RMPC is a control strategy well-suited for the systems subjected to physical and environmental constraints. One of the constraints exists in TWIP is the maximum torque produced by motors that can be regarded as control input constraint. According to (16), by tacking 40 N.m maximum torque for each motor, we have u_{max}=±80 N.m as input constraint for both "pendulum" and "rotation" subsystems. Figs 5 to 8 illustrate the performance of "pendulum" and "rotation" subsystems for $[\alpha \quad \dot{\alpha} \quad v \quad \theta \quad \dot{\theta}]$= [0.1750 0.0175 1 0 0] as initial condition for nominal system with u_{max}=±80 N.m as input constraint.

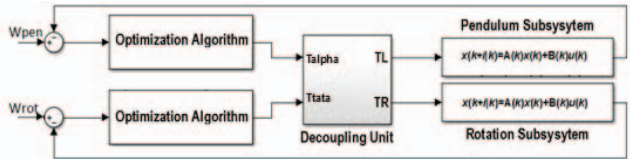

Figure 2. Block diagram of RMPC of the TWIP

Fig 5 illustrates the "rotation" subsystem to track the desired rotation angle θ_d=0.35rad=20degree. As seen, the yaw angle approaches desired angle in about 6 seconds. According to Fig 6 the control input needed for this action is less than u_{max}=±80 N.m. Figs 7 and 8 indicate that RMPC stabilize the "pendulum" subsystem in about 5 seconds, meanwhile the input control is limited to u_{max}=±80 N.m .

As noted earlier, tilt deviation makes the robot accelerate and decelerate until the specified speed is attained. In Figs 9 and 10, the performance of RMPC is illustrated for tracking the desired speed of 3 m/s with no constraint and u_{max}=±80 N.m as input constraint. It is seen that RMPC make the robot track the desired speed of 3 m/s during slightly more time.

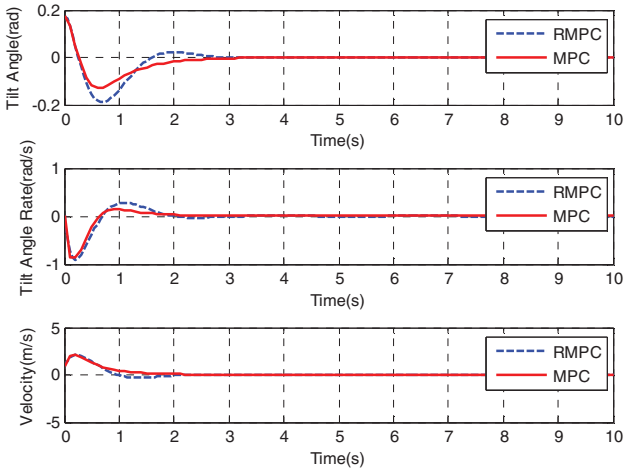

Figure 3. Performance of RMPC and nominal MPC in "pendulum" subsystem for nominal system with $[\alpha \quad \dot{\alpha} \quad v \quad \theta \quad \dot{\theta}]$= [0.1750 0.0175 1 0 0]as initial condition with no constraints

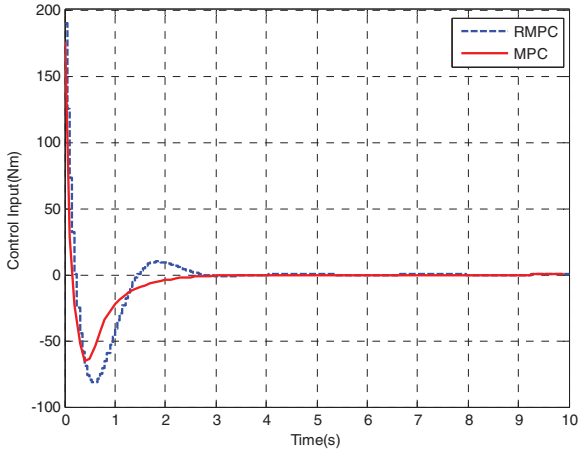

Figure 4. Control input of RMPC and nominal MPC in "pendulum" subsystem for nominal system with $[\alpha \quad \dot{\alpha} \quad v \quad \theta \quad \dot{\theta}]$= [0.1750 0.0175 1 0 0] as initial condition with no constraints

TABLE II. COMPARISON OF CONTROLLERS IN TERMS OF MSE ERROR

Method	RMPC		MPC	
System	Tilt Angle	Velocity	Tilt Angle	Velocity
nominal	0.0016	0.2023	0.0022	0.2805
1st vertex	0.0013	0.1960	0.0049	0.4173
3rd vertex	0.0014	0.1937	0.0050	0.4297
5th vertex	0.0014	0.1982	0.0056	0.4255
7th vertex	0.0014	0.2012	0.0058	0.4402
9th vertex	0.0019	0.2219	0.0083	0.5023
11th vertex	0.0019	0.2243	0.0075	0.5124
13th vertex	0.0020	0.2243	0.0077	0.5230
15th vertex	0.0020	0.2270	0.0088	0.5779

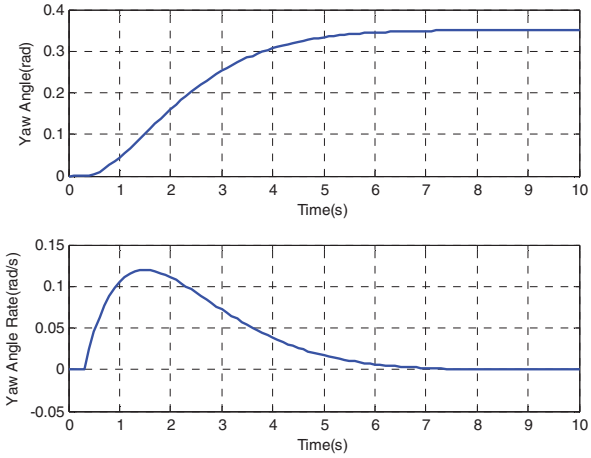

Figure 5. Performance of RMPC in "rotation" subsystem with $[\alpha \quad \dot{\alpha} \quad v \quad \theta \quad \dot{\theta}]$= [0.1750 0.0175 1 0 0]as initial condition and $[\alpha \quad \dot{\alpha} \quad v \quad \theta \quad \dot{\theta}]$=[0 0 0 0.35 0] as final condition with u_{max}=±80 N.m as input constraint

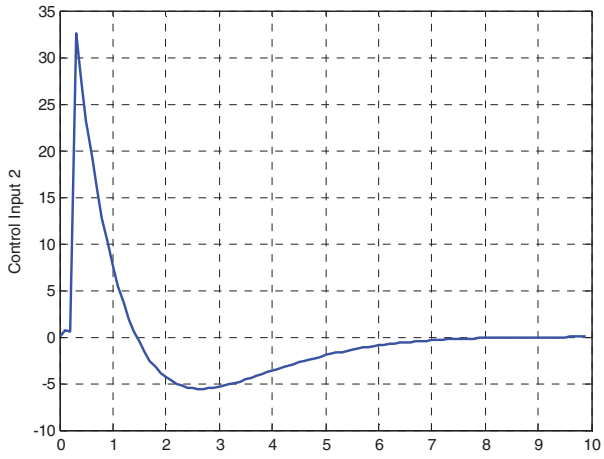

Figure 6. Control of RMPC in "rotation" subsystem for nominal system with $[\alpha \quad \dot{\alpha} \quad v \quad \theta \quad \dot{\theta}] = [0.1750 \quad 0.0175 \quad 1 \quad 0 \quad 0]$as initial condition and $[\alpha \quad \dot{\alpha} \quad v \quad \theta \quad \dot{\theta}] = [0 \quad 0 \quad 0 \quad 0.35 \quad 0]$ as final condition with u_{max}=±80 N.m as input constraint

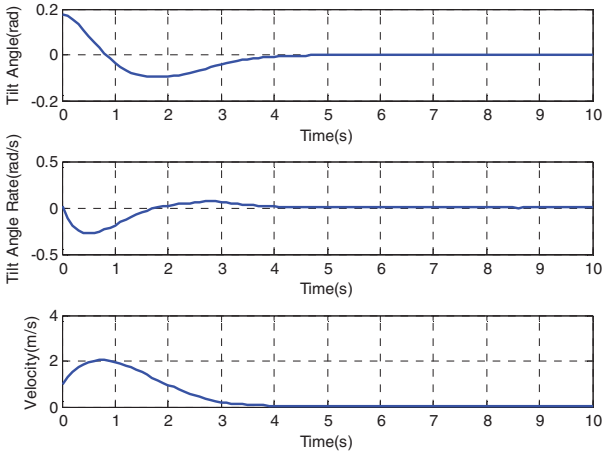

Figure 7. Performance of RMPC in "pendulum" subsystem for nominal system with $[\alpha \quad \dot{\alpha} \quad v \quad \theta \quad \dot{\theta}] = [0.1750 \quad 0.0175 \quad 1 \quad 0 \quad 0]$ as initial condition and $[\alpha \quad \dot{\alpha} \quad v \quad \theta \quad \dot{\theta}] = [0 \quad 0 \quad 0 \quad 0.35 \quad 0]$ as final condition with u_{max}=±80 N.m as input constraint

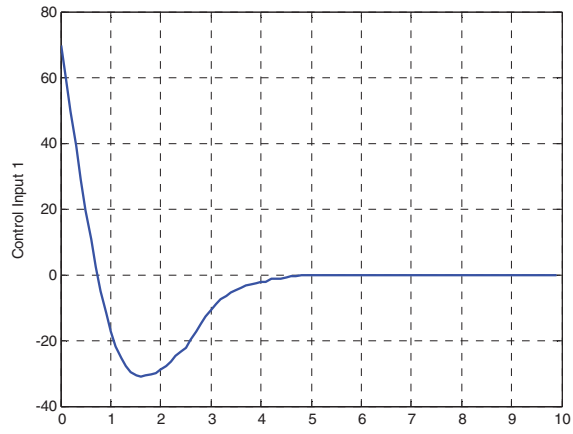

Figure 8. Control of RMPC in "pendulum" subsystem for nominal system with $[\alpha \quad \dot{\alpha} \quad v \quad \theta \quad \dot{\theta}] = [0.1750 \quad 0.0175 \quad 1 \quad 0 \quad 0]$ as initial condition and $[\alpha \quad \dot{\alpha} \quad v \quad \theta \quad \dot{\theta}] = [0 \quad 0 \quad 0 \quad 0.35 \quad 0]$ as final condition with u_{max}=±80 N.m as input constraint

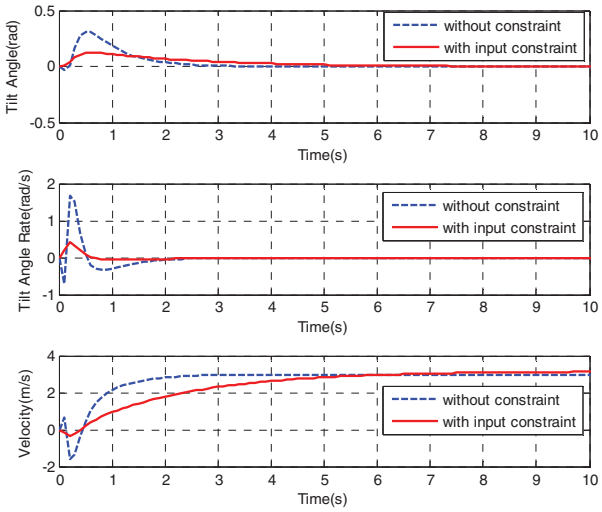

Figure 9. Performance of RMPC in "pendulum" subsystem for nominal system with zero initial condition and final speed of 3 m/s

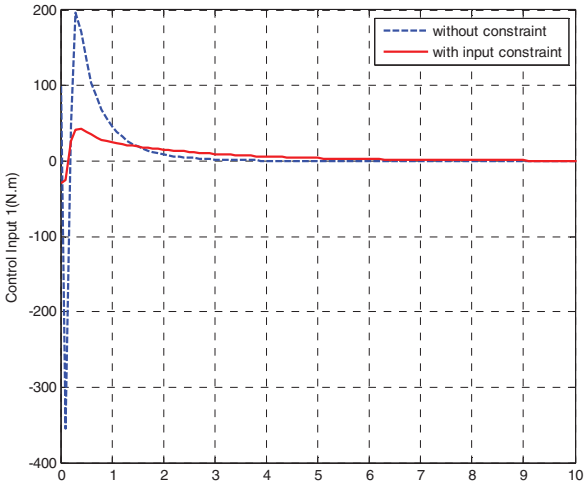

Figure 10. Control of RMPC in "pendulum" subsystem for nominal system with zero initial condition and final speed of 3 m/s

V. CONCLUSION

In this paper, two controllers are designed for stabilizing the posture of the TWIP using LMI-based RMPC method. RMPC is a control strategy optimizing "worst-case" objective function over infinite moving horizon, subject to input and output constraints. A parametric poly-topic uncertainty model is used to describe the robot. In a TWIP, model uncertainties stem from different mass and height of the pendulum that can cause uncertainties in moments of inertia about axes. Maximum torque produced by motors is defined as control input constraint. The efficiency of the RMPC is verified by comparing with nominal MPC. According to the results of the simulation, RMPC shows appropriate performance not only for the nominal system but also for the vertices of the poly-topic uncertainty model of the TWIP, whilst nominal MPC has the best performance for the nominal system. In addition, RMPC has been able to impose constraint on input control. As a conclusion, RMPC can be used to control the balancing and rotation of the TWIP in spite of the model uncertainties and input constrains.

REFERENCES

[1] Z. Li, C. Yang, and L. Fan, *Advanced control of wheeled inverted pendulum systems*: Springer, 2013.

[2] K. D. Do and G. Seet, "Motion control of a two-wheeled mobile vehicle with an inverted pendulum," *Journal of Intelligent & Robotic Systems,* vol. 60, pp. 577-605, 2010.

[3] B. Liu, M. Yue, and R. Liu, "Motion control of an underactuated spherical robot: A hierarchical sliding-mode approach with disturbance estimation," in *Mechatronics and Automation (ICMA), 2012 International Conference on*, 2012, pp. 1804-1809.

[4] M. Yue and X. Wei, "Dynamic balance and motion control for wheeled inverted pendulum vehicle via hierarchical sliding mode approach," *Proceedings of the Institution of Mechanical Engineers, Part I: Journal of Systems and Control Engineering,* vol. 228, pp. 351-358, 2014.

[5] F. Grasser, A. D'Arrigo, S. Colombi, and A. C. Rufer, "JOE: a mobile, inverted pendulum," *Industrial Electronics, IEEE Transactions on,* vol. 49, pp. 107-114, 2002.

[6] S. Nawawi, M. Ahmad, and J. Osman, "Real-time control of a two-wheeled inverted pendulum mobile robot," *World Academy of Science, Engineering and Technology,* vol. 39, pp. 214-220, 2008.

[7] C. Xu, M. Li, and F. Pan, "The system design and LQR control of a two-wheels self-balancing mobile robot," in *Electrical and Control Engineering (ICECE), 2011 International Conference on*, 2011, pp. 2786-2789.

[8] H. N. Nguyen, T. D. Huy, K. M. Tao, N. T. Phuong, and H. D. Loc, "Control Of Mobile Inverted Pendulum Using Sliding Mode Technique," *Ho Chi Minh City University of Technology (HUTECH), Vietnam, ISS_HUTECH–15/04,* 2010.

[9] M. Muhammad, S. Buyamin, M. N. Ahmad, and S. W. Nawawi, "Takagi-Sugeno fuzzy modeling of a two-wheeled inverted pendulum robot," *Journal of Intelligent and Fuzzy Systems,* vol. 25, pp. 535-546, 2013.

[10] C.-C. Tsai, S.-C. Lin, and B.-C. Lin, "Intelligent adaptive motion control using fuzzy basis function networks for self-balancing two-wheeled transporters," in *Fuzzy Systems (FUZZ), 2010 IEEE International Conference on*, 2010, pp. 1-6.

[11] D. Zhang, Q.-L. Han, and X. Jia, "Network-based H∞ fuzzy control for a self-balancing two-wheeled inverted pendulum," in *Industrial Electronics (ISIE), 2013 IEEE International Symposium on*, 2013, pp. 1-6.

[12] M. Azimi and H. Koofigar, "Model predictive control for a two wheeled self balancing robot," in *Robotics and Mechatronics (ICRoM), 2013 First RSI/ISM International Conference on*, 2013, pp. 152-157.

[13] N. Minouchehr and S. K. Hosseini-Sani, "Design of Model Predictive Control of Two-Wheeled Inverted Pendulum," in *Robotics and Mechatronics (ICRoM), 2015 The third RSI International Conference on*, 2015.

[14] M. V. Kothare, V. Balakrishnan, and M. Morari, "Robust constrained model predictive control using linear matrix inequalities," *Automatica,* vol. 32, pp. 1361-1379, 1996.

[15] K. Pathak, J. Franch, and S. K. Agrawal, "Velocity and position control of a wheeled inverted pendulum by partial feedback linearization," *Robotics, IEEE Transactions on,* vol. 21, pp. 505-513, 2005.

[16] M. Grant, S. Boyd, and Y. Ye, "CVX: Matlab software for disciplined convex programming," ed, 2008.